Carbon Exchange between the Atmosphere and Subtropical Forested Cypress and Pine Wetlands

W. Barclay Shoemaker[1], Frank Anderson[2], Jordan G. Barr[3], Scott L. Graham[4], and Daniel B. Botkin[5]

[1] U.S. Geological Survey, Florida Water Science Center, 7500 SW 36th St, Davie, FL 33314, bshoemak@usgs.gov, 954-377-5956

[2] U.S. Geological Survey, California Water Science Center, Placer Hall, 6000 J Street, Sacramento, CA, fanders@usgs.gov, 916-2783258

[3] South Florida Natural Resource Center, Everglades National Park, Homestead, FL 33030

[4] NIWA Taihoro Nukurangi, Riccarton, Christchurch, NZ

[5] Department of Biology, University of Miami, Coral Gables, FL, USA

Abstract

Carbon dioxide exchange between the atmosphere and forested subtropical wetlands is largely unknown. Here we report a first step in characterizing this atmospheric-ecosystem carbon (C) exchange, for cypress strands and pine forests in the Greater Everglades of Florida as measured with eddy covariance methods at three locations (Cypress Swamp, Dwarf Cypress and Pine Upland) for two years. Links between water and C cycles also are examined at these three sites, and methane emission measured only at the Dwarf Cypress site. Each forested wetland showed net C uptake from the atmosphere both monthly and annually, as indicated by net ecosystem exchange (NEE) of carbon dioxide (CO_2). For this study, NEE is the difference between photosynthesis and respiration, with negative values representing uptake from the atmosphere that is retained in the ecosystem or transported laterally via overland flow (unmeasured for this study). NEE was greatest at the Cypress Swamp (-900 to -1000 g C per m^2 year), moderate at the Pine Upland (-650 to -700 g C per m^2 year), and least at the Dwarf Cypress (-400 to -450 g C per m^2 year). Changes in NEE were clearly a function of seasonality in solar insolation, air temperature and flooding which suppressed heterotrophic soil respiration. We also note that changes in the satellite-derived enhanced-vegetation index (EVI) served as a useful surrogate for changes in -NEE at these forested wetland sites.

1 Introduction

At global scales, wetlands are generally considered sinks for atmospheric carbon dioxide (Troxler et al. 2013, Bridgham et al., 2006) and natural sources for methane emission (Whalen 2005, Sjogersten et al. 2014). Wetlands in southern Florida's greater Everglades (http://sofia.usgs.gov/) are expansive subtropical ecosystems that are carbon (C) accumulating over geologic time scales (Jones et al., 2014). Here we report a first step in characterizing modern rates of atmospheric-ecosystem carbon (C) exchange, for cypress strands and pine forests in the Greater Everglades of Florida.

In addition to the insight provided on the role of subtropical forested wetlands in the global carbon cycle, this research is expected to be useful for determining consequences of land-use changes in the Everglades region. Canal building and drainage projects in south Florida have reduced the original extent of the Everglades (Parker et al., 1955), decreased peat accretion rates and total carbon stocks, and reduced ecosystem services. Hohner and Dreschel (2015), for example, estimate the Greater Everglades has less than 24% its original peat volume and 19% of its original carbon. In response, State and Federal governments are planning and executing complex projects to restore Everglade's wetlands (http://www.evergladesplan.org/) while concurrently avoiding flooding in urbanized areas and maintaining water supply.

Restoring ecosystems will affect water, energy and C cycles, as plants and soil processes adjust to changing water levels, salinities, nutrient loads and fire regimes. For example, Jimenez et al. (2012) and Schedlbauer et al. (2010) indicate that additional deliveries of water into peat and marl saw grass wetlands may diminish C accumulation within these wetlands. Eddy-covariance derived estimates of net ecosystem productivity declined with increasing inundation during the wet season (Jimenez et al., 2012; Schedlbauer et al., 2010). These results were partially attributed to the amount of vegetation that, due to flooding, could not directly exchange carbon dioxide with the atmosphere. The opposite trend was observed in a tidally influenced mangrove forest in Everglades National Park. Lowered salinities, resulting from increased freshwater flow, resulted in increased daily PAR-use efficiency (i.e. ratio of gross ecosystem productivity to photosynthetically active irradiance (PAR), (Barr et al., 2010; Barr et al., 2012). Also, ecosystem respiration losses were lower during periods of inundation (Barr et al., 2010; Barr et al., 2012), which increased net C uptake over the mangrove forest. These studies provide insights on water and C cycling over coastal sawgrass wetlands and mangrove forests. C cycling over other subtropical wetlands, such as cypress strands and pine forests, is largely unstudied (Sjogersten et al. 2014).

The primary goal of this paper is to quantify the magnitude and controls of C exchange within cypress and pine forested wetlands. These wetland communities are defined by McPherson (1973) and Duever et al. (1986, 2002). Quantities of interest include net atmospheric/ecosystem C exchange (NEE), ecosystem respiration (RE), gross ecosystem exchange (GEE), and methane emissions. Latent heat flux (LE) and evapotranspiration (ET) also are quantified so that links between water and C cycles can be quantitatively studied. We address several specific objectives on daily, monthly and annual time scales, including (1) the magnitude of cypress (tall and dwarf) and pine forested wetlands as net atmospheric C sources or sinks, (2) site differences in water and C exchange metrics (i.e., -NEE, GEE, RE, and surface energy fluxes), and (3) the magnitude of methane emission over a dwarf cypress wetland. Results from this study are expected to help define and predict responses of subtropical forested wetlands to regional (e.g., freshwater discharge) and global (e.g., air temperature) environmental change.

2 Methods

2.1 Site Description

The study area is the Big Cypress National Preserve (BCNP) in southern Florida (Figure 1). A variety of subtropical forested and non-forested wetland ecosystems are present in BCNP, including Pine Upland, Wet Prairie, Marsh, Hardwood Hammocks, Cypress Swamps, Dwarf Cypress and Mangrove Forests as formally characterized by McPherson (1973) and Duever et al. (1986, 2002). The distribution of ecosystems and plant communities in the BCNP is controlled by topography, hydrology, fire regimes, and soil conditions (Duever et al., 1986). Marsh, Cypress Swamp, and Mangrove Forests typically occupy low elevations (< 2.5 m National Geodetic Vertical Datum, NGVD-29), Wet Prairie occupies middle elevations (3 to 4 m NGVD-29), and Pine Uplands and Hardwood Hammocks occupy high elevations (>4 m NGVD-29). These wetlands provide floodwater protection, hurricane buffering, substrate stabilization, sediment trapping, water filtration, and other ecosystem services for urban areas and coastal estuaries.

Water and C fluxes were determined over Pine Upland, Cypress Swamp and Dwarf Cypress ecosystems (Figure 1, Table 1) from December 2012 to November 2014 (Shoemaker et al., 2015d, e, f). The Pine Upland site (Figure 2, Table 1), is classified as a mixed lowland pine site, and is located in an extensive open-canopy pine forest with numerous small- to medium-sized cypress domes. The canopy is dominated by slash pine (*Pinus elliottii*) with an understory of saw palmetto (*Serenoa repens*), small trees and shrubs including holly (*Ilex cassine*), swamp bay (*Persea palustris*), myrsine (*Myrsine cubana*), and wax myrtle (*Myrica cerifera*), and scattered sabal palms (*Sabal palmetto*) (Figure 2). The ground cover is a diverse mix of short (less than 1 m) grasses, sedges, and forbs that are scattered in open-to-dense patches around the site. The open character of the site indicates regular burning with fire recurrence every 5 years, on average. Large cypress domes have a dense canopy of cypress, but open subcanopy and shrub strata, probably due to frequent fires. Substrates are primarily limestone bedrock, with sandy marl in the shallow depressions. Cypress domes in the area have a shallow organic substrate in the deeper areas.

The Cypress Swamp site (Figure 2, Table 1) is classified as a swamp forest (Duever et al., 1986) and supports a tall dense cypress forest with a subcanopy of mixed hardwoods (Figure 2). Plant varieties include bald cypress (*Taxodium distichum*), holly, swamp bay, maple (*Acer rubrum*), an open-to-dense shrub layer with coco plum (*Chrysobalanus icaco*), myrsine, wax myrtle, an open-to-dense ground cover of swamp fern (*Blechnum serrulatum*), and a variety of grasses, sedges, and forbs. The substrate is primarily topographically irregular limestone bedrock with organic accumulations in depressions in the rock.

The Dwarf Cypress site is classified as scrub cypress and is dominated by cypress, *Taxodium distichum*, and scattered (5 to 10 percent cover) sawgrass less than 1 m high (Figure 2). Small to medium-sized cypress domes are present, and periphyton is seasonally abundant (Figure 2) from about July to December. The substrate is shallow marl overlying topographically irregular limestone bedrock.

2.2 Carbon Balance

A mass balance equation can be used to conceptualize C fluxes. Net ecosystem C balance (NECB) is the amount of C accumulating in the ecosystem, in units of mass per area time (Chapin et al. 2006, Troxler et al., 2013). NECB can be partly approximated using eddy-covariance methods by measuring (1) the net vertical (1-dimensional) exchange of carbon dioxide (-NEE) across the ecosystem-atmosphere interface, (2) the net lateral flux (F_{net}) of dissolved/particulate organic/inorganic C leaving the system, and (3) the C released from methane emission (F_{CH4}):

$$NECB = -NEE - F_{net} - F_{CH4} \tag{1}$$

A negative sign for NEE indicates a loss of carbon dioxide from the atmosphere. The net lateral flux of C (F_{net}) occurs primarily within surface water that flows down topographic gradients toward mangrove wetlands on the coast (Figure 1). Technical difficulties inherent in measuring "sheet flow" and the dissolved/particulate organic/inorganic C concentrations within surface water did not allow quantification of this term. Therefore, we only report exchanges of gases between the atmosphere and the ecosystem. Methane emission (F_{CH4}) at the Dwarf Cypress site was determined using a LICOR-7700 open-path methane analyzer (Shoemaker et al., 2015d). The cost of the methane analyzer and safety issues related to climbing tall towers limited measurements of F_{CH4} to a single site (Dwarf Cypress, Figure 2). Thus, our daily and annual NEE estimates likely are an upper bound for C accumulation at the Pine Upland and Cypress Swamp sites (and lower bound for atmospheric transfer to the ecosystem) due to uncertainty associated with methane emission and lateral C fluxes.

2.3 Eddy Covariance Method and Gap-filling

The eddy covariance method (Dyer, 1961; Tanner and Greene, 1989) is a one-dimensional (vertical) approach for measuring the exchange of gases within the atmospheric surface layer (Campbell and Norman, 1998). Key instrumentation (Table 2) includes sonic anemometers that rapidly (10-Hz) measure wind velocity and gas analyzers that rapidly measure gas concentrations (Table 2) in the atmosphere. The covariance between vertical wind velocities and gas concentrations determines the net exchange of gases between the ecosystem and atmosphere. Additional instrumentation (Table 2) was installed at each site to measure net radiation, soil-heat flux, soil temperatures, air temperature and relative humidity, and distance of water above or below land surface (using pressure transducers). Pressure transducers were placed in the bottom of groundwater wells to measure the distance of water above and below land surface. Pressure transducers were corrected monthly for instrumentation drift using manual depth-to-water measurements from the top of the well casings. The manual depth-to-water measurements allowed precise calibration of continuous water distance above or below land-surface. Monthly site visits were made to download data, perform sensor inspections and complete other site maintenance. All instrumentation was visually inspected, leveled, cleaned, or replaced as necessary.

Raw, 10-Hz, vertical wind speed, temperature, and gas concentration data were processed to half-hourly fluxes using EddyPro software (version 4.0.0) following advanced protocols that included random uncertainty estimates (Finkelstein and Sims, 2001), spiking filters, double coordinate rotations, blocked-average detrending, statistical filters, air density and oxygen corrections (Tanner and Thurtell , 1969; Baldocchi et al., 1988; Webb et al., 1980; Tanner et al. 1993), and high-pass filtering. Processed data yielded half-hourly mean values of NEE, methane, sensible and latent heat fluxes that were filtered to remove periods with unrealistic fluxes (*Cypress Swamp* - latent heat fluxes >800 and <-100 watts m^{-2}, sensible heat flux >500 and <-150, NEE >25 and <-30 µmol m^{-2} s^{-1}; *Dwarf Cypress* - latent heat fluxes >600 and <-150 watts m^{-2}, sensible heat flux > 500 and <-100, NEE >20 and <-25 µmol m^{-2} s^{-1}, FCH4 >0.5 and <-0.2; *Pine Upland* - latent heat fluxes >1000 and <-300 watts m^{-2}, sensible heat >500 and <-200 watts m^{-2}, NEE >125 and <-100 µmol m^{-2} s^{-1}. These thresholds may inherently disregard some naturally large uptake or efflux events. For instance, ebullition events can be an important mechanism for episodic release of methane to the atmosphere (Comas and Wright, 2012). However, at present, the drivers of these events are not well understood and thus difficult to model with physiological-based gap-filling procedures.

Following EdiPro processing, local despike and friction velocity filters were applied to the gas fluxes (Shoemaker et al., 2015d, e, f). The local despike filter removed half-hour fluxes that fell outside 3 standard deviations of the fluxes within a moving 7-day window. Friction velocity is an indicator of time periods when turbulent wind conditions are well developed. Eddy covariance methods are appropriate for turbulent wind conditions. The u* threshold was selected based on plots of u* versus nighttime (9PM to 4AM) NEE normalized by air temperature and vapor pressure deficit, as described by Aubinet et al. (2012, pg. 147). NEE appeared to be considerably different as u* decreased approximately below 0.1 threshold. Roughly 25, 17, and 21 percent of NEE values were removed by the u*, local despike and unrealistic value filters at the Cypress Swamp, Dwarf Cypress and Pine Upland sites, respectively.

At the Pine Upland site, NEE contamination was possible due to fossil fuel combustion by generators and trucks supporting oil-drilling activities adjacent to the eddy-covariance tower. Thus, all carbon fluxes were removed at Pine Upland when the wind direction was from the east of the tower (15 to 130^o). This filter removed about 50% of the remaining NEE data, under the assumption the NEE fluxes were likely affected by drilling activities. East winds were evenly distributed over day (145^o mean wind direction) and night (167^o mean wind direction). Winds originated from the east mostly during the winter (October to December) as regional-scale cold fronts moved southward with winds blowing over peninsular Florida from the Atlantic Ocean towards the Gulf of Mexico. Nevertheless, over ten-thousand NEE fluxes remained for trend identification and gap-filling after the contamination filter at the Pine Upland site. Seasonal trends were apparent and diurnal NEE variations were resolvable into surrogates for respiration and photosynthesis, as described below.

Missing 30-minute fluxes (NEE, LE, H) were gap-filled using a look-up table approach (Table 3) documented in Reichstein (2005). The look-up table replaces missing fluxes with available fluxes collected during similar meteorological conditions (net radiation within 50 W m^{-2}, air temperature within 2.5 °C and vapor pressure deficit within 5.0 Pa). Gap-filled fluxes are grouped into "Filling Quality A, B, and C". To briefly summarize, "Filling Quality A" gap-fills based on the availability of various combinations of NEE, net radiation, air temperature and vapor pressure deficit data that meet similarity requirements within a 1-hour to 14-day gap-centered window. "Filling Quality B" gap-fills based on the availability of NEE, net radiation, air temperature and vapor pressure deficit data that meet similarity requirements within a 1 to 140-day gap-centered window. "Filling Quality C" gap-fills based on averages of available NEE data surrounding the gap. Reichstein (2005) contains further details regarding this gap-filling algorithm.

Positive NEE during the night was assumed to represent ecosystem respiration (RE). RE was weakly correlated with quantities such as air temperature (R^2 = 0.01 and 0.03 for linear and exponential regression at Cypress Swamp, for example); thus, a statistical model was used for predicting RE during the day. Daytime RE predictions were needed for gross ecosystem exchange (GEE) estimates. The statistical model randomly estimated values for day-time RE within one standard deviation of the mean RE over a day. For example, if 20 RE (+NEE) values were available within a 24-hour period, the mean and standard deviation of RE was computed using 20 available values. Subsequently, 28 daytime RE values were randomly predicted from a range that was one standard deviation from the mean. Assuming day-time and night-time respiration statistics are equal could be a source of error in our results. Identification of an alternative for the RE statistical model was precluded by weak correlations between respiration and ancillary variables such as air temperature.

Methane emissions (F_{CH4}) at the Dwarf Cypress site were most problematic in terms of missing 30-minute data. About 80% of the F_{CH4} time series was missing, mostly due to poor signal strength of the methane analyzer (signal strength filter <10). Furthermore, spikes in methane fluxes were removed when the signal strength indicator (RSSI) changed by +-10 between half-hourly time periods. Missing F_{CH4} fluxes were distributed evenly over day and night. Sub-daily gap-filling with the Reichstein (2005) lookup table and empirical regression models was confounded by weak correlations with explanatory data, the greatest being $R^2 = 0.11$ with barometric pressure. Correlations were similarly weak when isolating methane emissions between 10AM and 2PM; specifically, the greatest correlation ($R^2 = 0.12$) occurred with vapor pressure deficit. Given weak sub-daily correlations, over six-thousand molar methane fluxes were averaged by day and up-scaled to 357 molar fluxes of F_{CH4} at daily resolution.

Seasonally, missing daily F_{CH4} molar fluxes were more prevalent from 12/2012 to 5/2013; 10/2013 to 1/2014; 4/2014 to 5/2014; and 11/2014. Due to the seasonality of missing data, a molar flux model was constructed (daily resolution) as a power function of continuous variables that explained seasonality in methane emission, specifically, air temperature and flooding at the Dwarf Cypress site. The methane model was expressed as:

$$F_{CH_4} = R\ e^{(BT_a(1+e^{a+b(stage)}))} \qquad (2)$$

where T_a and *stage* were mean daily air temperature (Celsius) and water distance above (+) or below (-) land surface (meters), respectively. Least-squares regression defined values of

R=0.008628, *B*=0.04, *a*=-3.8, and *b*=2.7 that minimized sum-of-squared differences between observed and computed F_{CH4}molar fluxes (Figure 3). The F_{CH4} model explained about 40 percent of the variability in mean daily F_{CH4} fluxes.

Daily –NEE, RE, and F_{CH4} were converted from molar to mass units. Gross daily mass transfer of C from the atmosphere to the ecosystem (GEE, g C m^{-2} d^{-1}) was calculated as the sum of NEE and RE during the day. Daily GEE, -NEE, RE and F_{CH4} were summed to generate monthly and annual C exchange totals. An upper bound for uncertainty in these totals was approximated using a root mean square error propagating method (Topping, 1972). To summarize, possible sources of error included random uncertainty (Finkelstein and Sims, 2001) and gap-filling error. Gap-filling error was approximated using the standard error for ±NEE gap-filling by Reichstein (2005). Standard errors were computed by creating artificial gaps (1, 5, 10 and 20% removal) in observed NEE and predicting fluxes during the artificial gaps with the look-up table. The maximum standard error of the artificial gap scenarios was used to approximate an upper bound for uncertainty, as follows:

$$U_{-NEE,RE} = \sqrt{\sum_{t=0}^{month}(U_r^2 + SE_{max}^2)} \qquad (3)$$

where $U_{-NEE,RE}$ were monthly uncertainties in –NEE or RE in g C m^{-2} per month, U_r was random uncertainty (Finkelstein and Sims, 2001) in g C m^{-2} sec^{-1}, and $SE_{\max}$ was the maximum standard error of the artificial gap scenarios (20% removal scenario - equal to 2.2, 1.1, and 2.0 g C m^{-2} sec^{-1} for Cypress Swamp, Dwarf Cypress and Pine Upland, respectively). Uncertainty in monthly GEE was the sum of uncertainty for –NEE and RE. Uncertainty in F_{CH4} was estimated with Equation 3 using random uncertainty estimates (Finkelstein and Sims, 2001) for the methane fluxes and the standard error (equal to 0.017 g C m^{-2} d^{-1}) of the methane flux model (equation 2).

3 Results and Discussion

3.1 Seasonality in Rainfall, Temperature, Water Levels and Energy Fluxes

The subtropics of south Florida are characterized by distinct wet and dry seasons driven by changes in solar insolation, air temperature, humidity, and rainfall. Rainfall and photosynthesis are greatest in the hot and humid spring and summer months from about May to October. The end of October generally marks the end of the wet season (and hurricane season). Wetland water levels and surface energy fluxes are tightly coupled to seasonality in heat and humidity. Cold fronts are especially remarkable within surface energy budgets, as dry cold air passes over relatively warm soil and surface water, creating large variations in both stored-heat energy and turbulent fluxes of heat and water vapor (Shoemaker et al., 2011).

During this study, air temperatures at all three sites (Figure 4 A-C) were seasonally lowest (ranging from 15 to 25 ^{o}C) during December through March, and as low as 12 C for several days during the passage of cold fronts in the winter. Cold fronts typically lasted 5 days or less. During April and May, air temperatures rose above 25 C and were less variable as hot and humid air masses dominated the subtropical region. By late May, air temperatures were consistently 25 to 30 C and remained within this range until the onset of the dry season in mid-to-late October. Water and soil temperatures (measured 0.15 m below land surface) were nearly identical (absolute differences < 1 C) but were 1 to 5 C higher than air temperature during the passage of cold fronts (Figure 4). Land surface served as a heat reservoir during cold fronts, and water and soil temperatures seldom fell below 15 C. Cold fronts also increase vapor pressure deficits due to cold, dry air moving rapidly over relatively wet and warm landscape.

Seasonality was observed in water levels at each site (Figure 4A, B and C) in response to rainfall duration and intensity. Water levels were lower in the winter and early spring due to reduced rainfall at the end of the dry season (i.e., November to May). Water levels rose in response to rainfall at the end of April 2013 and May 2014, reaching ~1 m above land surface during July through October at the Dwarf Cypress site. In contrast, water levels declined as much as 1.0 m below land surface during the spring dry season from March to May 2014 (Figure 4A, B and C) creating an opportunity for enhanced soil respiration. Water levels remained below land surface until rainfall in June 2014 eventually flooded each site.

Surface energy fluxes reflected the seasonality in air temperature and rainfall (Figure 4A, B, C). Mean daily net radiation ranged from about 50 to over 200 W m^{-2} and was greatest in the summer months of June, July and August 2013 and 2014. Net radiation was least from November to February when incoming solar radiation was seasonally smallest. Net radiation was the primary driver of available energy and latent heat flux (Figure 4A, B, C), the energy equivalent of evapotranspiration (ET). Mean daily latent heat fluxes ranged from about 0 to over 150 W m^{-2} and were greatest in the summer months of June, July and August 2013 and 2014 at the Cypress Swamp site. Latent heat fluxes were lowest from November to February when incoming solar radiation was seasonally lowest, and less water was available for evaporation. During these cooler and drier periods, transpiration also was limited by lower physiological activity of trees, especially of the deciduous cypress trees (Figure 2B) during fall-winter leaf drop (Figure 4B). Surface inundation combined with more incoming solar radiation resulted in more energy partitioned as latent versus sensible heat during May to November. Also, cypress leaves were notably greener during this period suggesting increased physiological activity and seasonally higher transpiration rates.

3.2 Carbon Exchange between the Atmosphere and Forested Wetlands

All three sites were generally sinks of atmospheric carbon dioxide (CO_2) on daily, monthly (Figure 5A, B, C) and annual time scales (Table 4). The sink strength of CO_2 at each site, as evidenced by –NEE, was reduced during the fall and winter of 2012, 2013 and 2014

(Table 4, Figure 5). Seasonality in daily –NEE was least at Dwarf Cypress with –NEE ranging from -1.0 to -2 g C m^{-2} d^{-1} in the winter and summer, respectively. Seasonality in –NEE was more extreme Cypress Swamp and Pine Upland with rates ranging from -1 to -5 g C m^{-2} d^{-1} in the winter and summer, respectively. Lack of forested vegetation at Dwarf Cypress likely explains the dampened seasonality in C fluxes. Furthermore, pine trees grow and maintain leaves all year (evergreen trees), which likely explains dampened seasonality in –NEE at Pine Upland relative to Cypress Swamp.

The Moderate-resolution Imaging Spectroradiometer (MODIS) enhanced vegetation index (EVI) served as a useful qualitative surrogate for seasonal terrestrial photosynthetic activity and canopy structural variations (Figure 5), as reported for some other studies (Huete et al. 2002). EVI over tall mangrove forest, for example, varied seasonally between 0.35 and 0.55, and decreased to ~0.2 following defoliation after hurricane Wilma (Barr et al., 2013). Likewise, EVI over evergreen forest (Xiao et al. 2004a) varied seasonally between 0.25 during the winter and 0.5 during the summer growing season. EVI data were obtained from the MOD13A1 product of MODIS (EOS; http://modis.gsfc.nasa.gov/). Sixteen-day composite EVI values for the pixel corresponding to each station, and the 8 adjacent pixels were extracted for comparison with monthly C fluxes (Figure 5). This 9-pixel domain approximately corresponds with the measurement footprint of each flux station.

Seasonal patterns in –NEE and GEE were consistent with changes in EVI (Figure 5A, B, C), most notably at the Cypress Swamp site. Increases in EVI from 0.25 to 0.35 corresponded with growth of cypress leaves on relatively tall (18 to 21 m) and densely-spaced cypress trees (Figure 2) beginning in about March to April. Cypress leaves discontinued growing in August to September and turned brown in October, eventually falling into the sawgrass and hardwood understory. This lack of photosynthetic activity corresponded with changes in EVI from 0.4 in the summer to 0.2 in the winter (Figure 5B) of 2013 and 2014 at the Cypress Swamp flux station.

Gross atmosphere-ecosystem C exchange (GEE) provides a first approximation of gross ecosystem productivity (GEP), or accumulation of C in the plant canopy. Growth and senescence of cypress leaves was most evident in monthly GEE (Figure 5, Table 4) at the Cypress Swamp site, where rates increased from about 100 g C m^{-2} in February 2013 to over 200 g C m^{-2} in April 2013 (a 116 % increase). Likewise, GEE increased from about 100 g C m^{-2} in February 2014 to about 300 g C m^{-2} in June 2014 (a 200 % increase). At the Dwarf Cypress site, seasonal changes in GEE were more moderate; the February to April 2013 increase was from about 60 g C m^{-2} to 100 g C m^{-2} (a 66 % increase). Foliage change at the Cypress Swamp site likely contributed to a larger fraction of the site's change in photosynthetic CO_2 uptake compared to that of the Dwarf Cypress site, which consists of a sparse cypress canopy (Figure 2) during the height of the growing season (i.e., April to September).

A key water and ecosystem management issue in south Florida, and globally, is the preservation of organic soils within wetlands (Hohner and Dreschel, 2015) to (1) support ecosystem services, and (2) maintain or grow topography. Growing topography via C accumulation in these coastal forested wetlands could partly offset sea-level rise. Inundation suppressed respiration most remarkably at Cypress Swamp and Pine Upland (Figure 5A, B). RE doubled from about 60 to 120 g C m^{-2} from February to May 2014 when water levels were below land surface at Cypress Swamp (Figure 5B). Enhanced RE also was observed from March 2014 to July 2014 at Pine Upland (Figure 5A) when water levels were below land surface. Enhanced RE was likely due to heterotrophic soil respiration supplementing autotrophic respiration when water levels were below land surface for extended periods of time. These results suggest hydroperiod could be managed for maintenance of organic soils and peat accretion in these subtropical cypress and pine forested wetlands.

3.3 Links between C and Water Cycles

Relationships between net ecosystem C exchange (-NEE) and latent heat flux (LE) reflect an important link between water and C cycles (Figure 6); that is, photosynthesis that releases water (transpiration) while storing C. R^2 between –NEE and LE provides an indication of the relative magnitudes of transpiration and evaporation at each site. Stronger correlations between NEE and LE indicate increased transpiration relative to evaporation, as water is transpired during photosynthesis while the plant fixes C. In contrast, weaker correlations indicate a site with more open water evaporation where the source for ET is less related to photosynthesis and more related to evaporation from a water surface. Correlations between –NEE and LE were 0.35, 0.36 and 0.19 (Figure 6) at the Cypress Swamp, Pine Upland and Dwarf Cypress sites, respectively. These correlations indicate transpiration is a larger portion of evapotranspiration at the forested wetlands with larger and more densely spaced cypress and pine trees. Closed or partially closed forested canopies reduced penetration of solar radiation to water surfaces, creating lowered lapse rates between the water surface and canopy crown (Barr et al., 2012), and added resistance to evaporation. Collectively, these results indicate a redistribution of plant communities toward more open-water ecosystems (such as sparse sawgrass) could result in less C uptake and greater evaporative losses. Prior studies of C accumulation further support this generalization; for example, NEE rates were greater over mangrove systems (Barr et al., 2010; Barr et al., 2012) than over sawgrass wetlands (Schedlbauer et al., 2010). Furthermore, prior ET studies (German, 2000) indicate ET losses are greater over wetlands with sparse sawgrass and open-water conditions.

Coupling between water and C cycles was examined via water-use efficiencies (Table 5) computed as the ratio of annual NEE to ET. As such, WUE are the net mass or moles of C transferred to the ecosystem per mm or mole of water vapor. Computing WUE with NEE accounts for the loss of C through Re. The Cypress Swamp and Pine Upland sites were most efficient at using water to store C, with WUE equal to about 1.0 g C per mm ET (1.0 to 1.4 moles CO_2 per mole of ET). About 0.5 g C uptake occurs per mm of ET (0.7 moles CO_2 per mole of ET) at the Dwarf Cypress site. Apparently, wetlands with more open-water surface (Figure 2) are less efficient than forested wetlands at converting water use into net and gross C uptake. This conclusion is likely to be true both regionally and perhaps globally, and thus, may have implications for the global C cycle.

3.3 Methane Emission

Methane is produced by anaerobic bacteria decomposing organic matter in the soil or surface water. Methane can be oxidized during transport from the soil or surface water into the atmosphere. Transport to the atmosphere may occur through (1) roots and stems of vascular plants (Wang and Han, 2005; Morrissey et al., 1993; Kim and Verma, 1998), (2) ebullition as gas bubbles from anaerobic soils (Comas and Wright, 2012), and (3) diffusion through the soil and surface water (Van Huissteden et al., 2006, Christensen et al., 2003a,b). Methane emission is enhanced as anaerobic bacteria become more active at higher temperatures (Simpson et al., 1995).

At the Dwarf Cypress site, methane emission increased with increasing air temperature and water level in the summer months from June to September 2013 (Figure 5C). In contrast, methane emission was suppressed from April to June 2014 due to dry conditions and perhaps the memory of dry conditions from July to September 2014. Anaerobic bacteria may take some time to reestablish following dry conditions. This reestablishment or “memory” of dry conditions would reduce methane emission despite warm conditions and flooding from July to September 2014.

Methane emission peaked at different times in the summer of 2013 compared to GEE at the Dwarf Cypress site (Figure 5C). GEE peaked with photosynthesis in July 2013 whereas methane emission peaked in August 2013. This time lag indicates that processes governing C exchange and methane emissions are quite different, with GEE controlled by photosynthesis of cypress leaves and sawgrass which grow vigorously from March to April and discontinue growth in August to September. In contrast, methane emission is driven by anaerobic decomposition of organic matter with subsequent oxidation through the soil and surface water. Organic decomposition was enhanced in August 2013 by flooding and relatively warm air, soil and surface-water.

Although methane emission is important in terms of global warming potential (GWP), it appears to be immaterial in C budgets that alter or “grow” land surface topography. C released from methane emission was relatively small (averaging about 10 g C per year) compared to NEE (about -500 g C per m^2 year, Table 4). Thus, C cycling studies that address changes in peat accumulation may not benefit from monitoring methane fluxes. However, about 14 g CH_4 emission per year is roughly equivalent to 350 g CO_2, assuming the GWP of CH_4 is 25 times greater than CO_2 (over a 100-year period, IPCC 2007). We recognize GWP multipliers are controversial due to assumptions such as instantaneous CH_4 and CO_2 release, and time-scale dependence of the radiative forcing contributions (Mitsch et al., 2013). Careful use of GWP multipliers for wetlands is suggested.

3.4 Comparison of C Uptake with Prior Studies

Comparison of our results with –NEE from selected prior studies (Schedlbauer et al. 2010; Jimenez et al. 2012; Barr et al. 2010; Botkin et al. 1970; Jones et al. 2014) reveals substantial spatial and temporal heterogeneity in C uptake over geologic time and among different ecosystems (Table 6). Subtropical forested wetlands exchange more C than temperate forests (Botkin et al., 1970; Sjogersten et al. 2014). A study assessing C exchange on a geologic time scale (Jones et al. 2014) also concluded that long-term rates of C uptake in the Everglades are higher than in northern latitudes, and in some cases rival C uptake in tropical peat-lands, such as Indonesia. Mangrove ecosystems may serve as an upper limit for subtropical C uptake, with NEE of about -1170 g C per m^2 year (Barr et al. 2010).

Sparse sawgrass wetlands in the Everglades, such as Taylor and Shark River Sloughs, are relatively minor atmospheric C sources or sinks, with –NEE ranging from -50 (Taylor Slough) to +45 (Shark River Slough) g C per m^2 year (Table 5). Jones et al. (2014) also concluded that sloughs sequester the least amount of C in their study of C accumulation over geologic time scales. Given the C released from methane emissions (10 g C per m^2 year, Table 4), as measured at Dwarf Cypress (Figure 5C), sparse sawgrass wetlands may generally be atmospheric C sources at monthly and annual time scales, with questionable value as local, regional and global C sinks.

4 Conclusions

Atmospheric/ecosystem carbon dioxide exchange, methane emission, latent and sensible heat fluxes were estimated with eddy covariance methods for subtropical forested cypress and pine wetlands for two years. Seasonality in solar insolation, air temperature, plant physiological activity, rainfall and water levels created seasonality in C exchange rates and surface energy fluxes. Links between water and C fluxes also were revealed such as photosynthetic water-use efficiencies.

Each forested wetland was an atmospheric C sink on monthly and annual time scales. NEE was greatest at Cypress Swamp (-900 to -1000 g C per m^2 year), moderate at Pine Upland (-650 to -700 g C per m^2 year), and least at Dwarf Cypress (-400 to -450 g C per m^2 year). The size (about 20 m) and number of cypress trees enhanced C uptake at Cypress Swamp and seasonality in C uptake rates was enhanced by the growth of cypress leaves in early April and decay of cypress leaves in late October, as confirmed by changes in the satellite-derived EVI. Changes in EVI (from 0.25 in the dry season to 0.4 in the wet season) served as a useful surrogate for monthly and seasonal changes in net and gross ecosystem C exchange.

Respiration was enhanced when water levels dropped below land surface within these cypress and pine forested wetlands. Increases in respiration were likely due to heterotrophic soil respiration supplementing autotrophic respiration. These results highlight the importance of flooding and hydro-period management for maintaining organic soils and peat accretion within subtropical forested wetlands, a key water and ecosystem management issue in south Florida and globally.

Links between water and C cycles were examined via (1) water-use efficiencies (WUE) expressed as the ratio of annual NEE to ET, and (2) correlations between -NEE and LE. Computing WUE with NEE accounts for the loss of C through respiration. The Cypress Swamp and Pine Upland sites were most efficient at using water to store C, with WUE equal to about 1.0 g C per mm ET. About 0.5 g C was stored in the ecosystem per mm of ET at the Dwarf Cypress site. These results indicate that wetlands with more open-water surface are less efficient at using water to store C than forested wetlands. This pattern is likely to be true both regionally and perhaps globally, and thus, may have implications for the global C cycle.

Correlations between -NEE and LE reflected photosynthesis which released water as transpiration while storing C. The strength of the –NEE and LE correlation provided an indication of the relative magnitudes of transpiration and evaporation at each site. Transpiration was a large proportion of evapotranspiration at the Cypress Swamp and Pine Upland sites, as indicated by correlations of 0.34, 0.36 and 0.18 for the Cypress Swamp, Pine Upland and Dwarf Cypress sites, respectively. These results indicate that a redistribution of plant communities toward more open-water ecosystems could create less C uptake and greater evaporative losses.

Methane emission at Dwarf Cypress was considerable in terms of global warming potential, but immaterial in C budgets that build and maintain land-surface topography. Approximately 14 g CH_4 was released into the atmosphere, roughly equivalent to 350 g CO_2, assuming the global warming potential of CH_4 is about 25 times greater than CO_2. Methane emission, however, did not reverse carbon accumulation for topography at Dwarf Cypress, as the C released from methane emission (about 10 g C per m^2 year) was relatively small compared to NEE (-500 g C per m^2 year). These results indicate that while methane monitoring is needed when assessing the global warming potential of wetlands; C cycling studies that address changes in topography and peat accumulation may not benefit from monitoring methane fluxes.

5 Acknowledgements

This study was funded, in part, by the U.S. Geological Survey (USGS) Greater Everglades Priority Ecosystems Science (GEEES). Nick Aumen is gratefully acknowledged for helpful conversations about the Everglades during project meetings and fieldwork in BCNP. Michael J. Duever provided detailed vegetation descriptions and guidance during site selection. Steve Krupa and Cynthia Gefvert from the South Florida Water Management District funded tower construction. USGS peer reviews by Lisamarie Windham-Myers, Dave Sumner and Kim

Haag improved the quality of the manuscript. Biogeoscience peer reviews by Ankur Desai and an anonymous referee also greatly improved the manuscript. Any use of trade, firm, or product names is for descriptive purposes only and does not imply endorsement by the U.S. Government.

6 References

Alberto, M.C.R., Carmelita R., R. Wassmann, R.J. Buresh, J.R. Quilty, T.Q. Correa, J.M. Sandro, Centeno C.A.R.: Measuring methane flux from irrigated rice fields by eddy covariance method using open-path gas analyzer, Field Crops Research 160 (2014) 12–21, 2014.

Baldocchi, D.D., Hicks, B.B., and Meyers, T.P.: Measuring biosphere-atmosphere exchanges of biologically related gases with micrometeorological methods: Ecology, v. 69, no. 5, p. 1331-1340, 1988.

Barr, J.G., V.C. Engel, J.D. Fuentes, J.C. Zieman, T.L. O'Halloran, T.J. Smith III, and G.H. Anderson G.H.: Controls on mangrove forest-atmosphere carbon dioxide exchanges in western Everglades National Park. Journal of Geophysical Research 115, G02020, http:// dx.doi.org/10.1029/2009JG001186, 2010.

Barr, J.G., V. Engel, T.J. Smith, and Fuentes J.D.: Hurricane disturbance and recovery of energy balance, CO2 fluxes and canopy structure in a mangrove forest of the Florida Everglades. Agricultural and Forest Meteorology 153:54–66, http://dx.doi.org/ 10.1016/j.agrformet.2011.07.022., 2012.

Barr, J.G., V. Engel, J.D. Fuentes, D.O. Fuller, Kwon H.: Modeling light-use efficiency in a subtropical mangrove forest equipped with CO2 eddy covariance. Biogeosciences, 10, 2145–2158, doi:10.5194/bg-10-2145-2013, 2013.

Botkin DB, GM Woodwell and Tempel N.: Forest productivity estimated from carbon dioxide uptake, Ecology Volume 51, No. 6, 1057 – 1060, 1970.

Bridgham, S. D., J. P. Megonigal, J. K. Keller, N. B. Bliss, and Trettin C.: The carbon balance of North American wetlands. Wetlands 26:889–916, 2006.

Campbell, G.S., and Norman, J.M.: An introduction to environmental biophysics: New York, Springer, 286 p., 1998.

Comas, X., and Wright W.: Heterogeneity of biogenic gas ebullition in subtropical peat soils is revealed using time-lapse cameras, Water Resour. Res., 48, W04601, doi:10.1029/2011WR011654, 2012.

Chapin, F.S., G.M. Woodwell, J.T. Randerson, E.B. Rastetter, G.M. Lovett, D.D. Baldocchi, D.A. Clark, M.E. Harmon, D.S. Schimel, Valentini R.: Reconciling carbon- cycle concepts, terminology, and methods. Ecosystems 9:1,041–1,050, http://dx.doi.org/ 10.1007/s10021-005-0105-7, 2006.

Christensen, T.R., Panikov, N., Mastepanov, M., Joabsson, A., Stewart, A., Oquist, M.,Sommerkorn, M., Reynaud, S., Svensson, B.: Biotic controls on CO2andCH4exchange in wetlands—a closed environment study. Biogeochemistry 64,337–354, 2003a.

Christensen, T.R., Ekberg, A., Strom, L., Mastepanov, M., Panikov, N., Mats, O., Svens-son, B.H., Nykanen, H., Martikainen, P.J., Oskarsson H.: Factors controllinglarge scale variations in methane emissions from wetlands. Geophys. Res. Lett.30, http://dx.doi.org/10.1029/2002L016848, 2003b.

Comas, X., and Wright W.: Heterogeneity of biogenic gas ebullition in subtropical peat soils is revealed using time-lapse cameras, Water Resour. Res., 48, W04601, doi:10.1029/2011WR011654, 2012.

Duever, M.J, Carlson, J.E. Meeder, J.F., Duever, L.C., Gunderson, L.H. Riopelle, L.A., Alexander, T.R., Myers, R.L., and Spangler, D.P.: The Big Cypress National Preserve: New York, National Audubon Society, 455 p., 1986.

Duever, M.J.: Southwest Florida Predevelopment Vegetation Map, Map Publication of the South Florida Water Management District, 1 p., 2002.

Dyer, A.J.: Measurements of evaporation and heat transfer in the lower atmosphere by an automatic eddy covariance technique: Quarterly Journal of the Royal Meteorological Society, v. 87, p. 401-412, 1961.

Finkelstein, P. L., and Sims, P. F.: Sampling error in eddy correlation flux measurements. Journal of Geophysical Research, 106: 3503-3509, 2001.

German, E.R.: Regional evaluation of evapotranspiration in the Everglades: U.S. Geological Survey Water Resources Investigations Report 00–4217, 48 p., 2000.

Hohner, S.M., Dreschel T.W.: Everglades peats: using historical and recent data to estimate predrainage and current volumes, masses and carbon contents, Mires and Peat, Volume 16 (2015), Article 01, 1–15, http://www.mires-and-peat.net/, ISSN 1819-754X, 2015.

Huissteden JV, R. van den Bos, Alvarez I.M.: Modelling the effect of water table management on CO2 and CH4 fluxes from peat soils Neth. J. Geosci.: Geol. En Mijnbouw, 85, 2006. pp. 3–18., 2006.

Huete, A., K. Didan, T. Miura, E.P. Rodriguez, X. Gao, and Ferreira L.G.: Overview of the radiometric and biophysical performance of the MODIS vegetation indices: Remote Sensing of Environment, v. 83, no. 1, p. 195-213, 2002.

Jimenez, K.L., G. Starr, C.L. Staudhammer, J.L. Schedlbauer, H.W. Loescher, S.L. Malone, and Oberbauer S.F.: Carbon dioxide exchange rates from short- and long-hydroperiod Everglades freshwater marsh. Journal of Geophysical Research 117, G04009, http://dx.doi.org/10.1029/2012JG002117, 2012.

Jones, M.C., C.E. Bernhardt, Willard D.A.: Late Holocene vegetation, climate and land-use impacts on carbon dynamics in the Florida Everglades, Quaternary Science Reviews 90 (2014) 90-105, 2014.

Kim J., Verma S.B.: Diel variation in methane emission from a midlatitudeprairie wetland: significance of convective through flow in Phragmites australis.J. Geophys. Res. 103, 29–39, 1998.

Mitsch W.J., Bernal B, Nahlik A.M., et al.: Wetlands, carbon, and climate change. Landscape Ecology 28:583–597. doi: 10.1007/s10980-012-9758-8, 2013.

McPherson, B.F.: Vegetation map of southern parts of subareas A and C, Big Cypress Swamp, Florida: U.S. Geological Survey Hydrologic Atlas HA-492, 1973.

Morrissey, L.A., Zobel, D.B., Livingston, G.P.: Significance of stomatal control on methane release from Carex-dominated wetlands. Chemosphere 26, 339–355, 1993.

Parker G.G., G.E. Ferguson, and Love S.K.: Water resources of southeastern Florida, with special reference to the geology and ground water of the Miami area, U.S. Geol. Surv. Water Supply Pap., 1255, 965 pp., 1955.

Priestley, C.H.B., and Taylor R.J.: On the assessment of surface heat flux and evaporation using large scale parameters: Monthly Weather Review, no. 100, p. 81–92, 1972.

Reichstein, M., E. Falge, D. Baldocchi, D. Papale, M. Aubinet, P. Berbigier, and R. Valentini.: On the separation of net ecosystem exchange into assimilation and ecosystem respiration: review and improved algorithm. Global Change Biology, 11(9): 1424-1439, 2005.

Schedlbauer, J., S. Oberbauer, G. Starr, and Jimenez K.L.: Seasonal differences in the CO2 exchange of a short-hydroperiod Florida Everglades marsh. Agricultural and Forest Meteorology 150:994–1,006, http://dx.doi.org/ 10.1016/j.agrformet.2010.03.005, 2010.

Shoemaker, W.B., and Sumner D.M.: Alternate corrections for estimating actual wetland evapotranspiration from potential evapotranspiration: Wetlands, v. 26, no. 2, p. 528–543, 2006.

Shoemaker, W.B., and Lopez, C.D., and Duever M.: Evapotranspiration over spatially extensive plant communities in the Big Cypress National Preserve, southern Florida, 2007–2010: U.S. Geological Survey Scientific Investigations Report 2011–5212, 46 p., 2011.

Shoemaker W. B., Anderson F., Barr J. G., Graham S. L., and Botkin D. B.: Carbon exchange between the atmosphere and subtropical forested cypress and pine wetlands, U.S. Geological Survey, Data Set for the Dwarf Cypress site, doi:10.5066/F7ZG6Q94, 2015d.

Shoemaker W. B., Anderson F., Barr J. G., Graham S. L., and Botkin D. B.: Carbon exchange between the atmosphere and subtropical forested cypress and pine wetlands, U.S. Geological Survey Data Set for the Cypress Swamp site, doi:10.5066/F73776RZ, 2015e.

Shoemaker W. B., Anderson F., Barr J. G., Graham S. L., and Botkin D. B.: Carbon exchange between the atmosphere and subtropical forested cypress and pine wetlands, U.S. Geological Survey Data Set for the Pine Upland site, doi:10.5066/F7707ZG9, 2015f.

Simpson I.J., G.W. Thurtell, G.E. Kidd, M. Lin, T.H. Demetriades-Shah, I.D. Flitcroft, E.T. Kanemasu, D. Nie, K.F. Bronson H.U.: Tunable diode laser measurements of methane fluxes from an irrigated rice paddy field in the Philippines J. Geophys. Res., 100 (1995), pp. 7283–7290, 1995.

Sjögersten S., C.R. Black, S. Evers, J. Hoyos-Santillan, E.L. Wright, and Turner B.L.: Tropical wetlands: a missing link in the global carbon cycle? American Geophysical Union doi: 10.1002/2014GB004844.

Tanner, B.D. and Greene J.P.: Measurement of sensible heat and water vapor fluxes using eddy correlation methods: Final report prepared for U.S. Army Dugway Proving Grounds, Dugway, Utah, 1989.

Tanner, C.B., and Thurtell G.W.: Anemoclinometer measurements of Reynolds stress and heat transport in then atmospheric surface layer: University of Wisconsin Technical Report ECOM-66- G22-F, 82 p., 1969.

Tanner, B.D., Swiatek, E., and Greene J.P.: Density fluctuations and use of the krypton hygrometer in surface flux measurements: Management of irrigation and drainage systems: Irrigation and Drainage Division, American Society of Civil Engineers, July 21-23, 1993, Park City, Utah, p. 945-952, 1993.

Topping, J.: Errors of Observation and Their Treatment. 4th ed. London, U.K.: Chapman and Hall, 1972.

Troxler, T.G., E. Gaiser, J. Barr, J.D. Fuentes, R. Jaffé, D.L. Childers, L. Collado-Vides, V.H. Rivera-Monroy, E. Castañeda-Moya, W. Anderson, R. Chambers, M. Chen, C. Coronado-Molina, S.E. Davis, V. Engel, C. Fitz, J. Fourqurean, T. Frankovich, J. Kominoski, C. Madden, S.L. Malone, S.F. Oberbauer, P. Olivas, J. Richards, C. Saunders, J. Schedlbauer, L.J. Scinto, F. Sklar, T. Smith, J.M. Smoak, G. Starr, R.R. Twilley, Whelan K.: Integrated carbon budget models for the Everglades terrestrial-coastal-oceanic gradient: Current status and needs for inter-site comparisons: Oceanography, 26(3), 98-107, 2013.

Twine, T.E., Kustas, W.P., Norman, J.M., Cook, D.R., Houser, P.R., Meyers, T.P., Prueger, J.H., Starks, P.J., Wesely M.L.: Correcting eddy-covariance flux underestimates over a grassland. Agricultural and Forest Meteorology 103, 279–300, 2000.

Huissteden V., J., van den Bos, R., Alvarez I.M.: Modelling the effect of watertable management on CO2and CH4fluxes from peat soils. Neth. J. Geosci.: Geol.En Mijnbouw 85, 3–18, 2006.

Wang, Z.P., Han X.G.: Diurnal variation in methane emissions in relationto plants and environmental variables in the Inner Mongolia marshes. Atmos.Environ. 39, 6295–6305, 2005.

Webb, E.K., Pearman, G.I., Leuning R.: Correction of flux measurements for density effects due to heat and water vapour transfer. Quarterly Journal of the Royal Meteorological Society 106, 85–100, 1980.

Whalen S.C.: Biogeochemistry of methane exchange between natural wet-lands and the atmosphere. Environ. Eng. Sci. 22, 73–94, 2005.

Xiao, X., D. Hollinger, J.D. Aber, M. Goltz, E. Davidson, Q. Zhang, and B. Moore III.: Modeling gross primary production of temperate deciduous broadleaf forest using satellite images and climate data. Remote Sensing of Environment 91 (2004) 256 – 270, 2004a.

Table 1. Site locations, tower heights and summary of vegetation.

Site	Latitude	Longitude	Height of tower (m)	Height of vegetation (m)	Vegetation
Dwarf Cypress	25.7624	-80.8934	16.8	0.5 to 10	Small cypress and sawgrass
Cypress Swamp	25.8265	-81.1020	38.1	0.5 to 21	Tall cypress
Pine Upland	26.0004	-80.9260	38.1	0.5 to 21	Pine, sawgrass and cypress

Table 2. Instrumentation installed at the Dwarf Cypress, Cypress Swamp and Pine Upland flux stations.

			Distance above or below land surface, in meters		
Instrument	**Model**	**Measurement**	**Dwarf Cypress**	**Pine Upland**	**Cypress Swamp**
Sonic anemometer	CSAT[1], Gill Windmaster Pro[2]	Wind velocity and direction	15.5	35.8	35.7
Gas analyzer	LI-7500A	Gas concentrations	15.5	35.8	35.7
Methane analyzer	LI-7700	Methane concentration	15.5	NA	NA
Pressure transducer	CS450	Water depth	-0.8	-0.5	-0.5
Air temperature	HMP-45C	Air temperature	15.5	35.8	35.8
Relative humidity	HMP-45C	Relative humidity	15.5	35.8	35.8
Net radiometer	NR-Lite	Net radiation	13.2	33.7	33.9
Soil heat flux	REB's	Soil heat flux	-0.2	-0.2	-0.2
Soil temperature	107L	Soil temperature	-0.2	-0.2	-0.2

[1] CSAT deployed at the Dwarf Cypress and Pine Upland sites.

[2] Gill Windmaster Pro deployed at the Cypress Swamp site.

Table 3. Gap-filling results for fluxes based on the look-up table approach by Reichstein et al. (2005).

Cypress Swamp	**H**[1]	**LE**[2]	**NEE**
Filling Quality A	8239	10591	11506
Filling Quality B	32	34	31
Filling Quality C	9	9	13
Total gap-filled	8280	10634	11550
Total fluxes	34848	34848	34848
Percent rejected	24	31	33
Dwarf Cypress	**H**	**LE**	**NEE**
Filling Quality A	6830	8365	9828
Filling Quality B	389	398	393
Filling Quality C	70	70	74
Total gap-filled	7289	8833	10295
Total fluxes	35328	35328	35328
Percent rejected	21	25	29
Pine Upland	**H**	**LE**	**NEE**
Filling Quality A	9001	9997	23554
Filling Quality B	138	139	174
Filling Quality C	243	242	393
Total gap-filled	9382	10378	24121
Total fluxes	35424	35424	35424
Percent rejected	26	29	68

[1] Sensible heat flux. [2] Latent heat flux.

Table 4. Monthly and annual C and methane fluxes.

	Cypress Swamp			**Dwarf Cypress**				**Pine Upland**		
Month	**-NEE[1]**	**Re[1]**	**GEE[1]**	**-NEE[1]**	**Re[1]**	**GEE[1]**	**CH_4[1]**	**-NEE[1]**	**Re[1]**	**GEE[1]**
Dec-12	-19±4	31±2	49±6	-18±1	27±1	45±3	0.6±0.003	-52±3	45±6	96±10
Jan-13	-30±5	51±2	81±8	-25±1	35±3	59±5	0.6±0.004	-54±4	63±6	117±10
Feb-13	-31±4	57±2	87±6	-22±4	43±3	65±7	0.5±0.003	-40±4	60±11	100±15
Mar-13	-75±3	83±2	157±5	-27±2	39±2	66±5	0.5±0.002	-59±4	69±8	127±12
Apr-13	-98±5	117±3	215±8	-50±3	45±4	94±7	0.6±0.003	-62±5	82±14	143±20
May-13	-123±5	99±3	221±9	-61±3	45±3	106±6	0.6±0.006	-89±5	64±13	152±19
Jun-13	-131±5	68±3	199±8	-58±5	43±3	101±8	1.1±0.005	-88±6	56±20	143±26
Jul-13	-107±5	51±3	157±9	-59±3	43±1	102±4	1.5±0.006	-103±6	54±22	157±29
Aug-13	-96±6	53±4	149±10	-45±3	37±3	82±7	2.3±0.011	-82±4	41±15	122±19
Sep-13	-67±6	61±3	128±10	-32±4	36±4	68±8	2±0.004	-45±4	58±11	103±16
Oct-13	-51±4	55±2	106±7	-27±2	28±1	55±4	1.7±0.004	-29±3	44±9	73±13
Nov-13	-42±5	61±3	103±15	-24±2	32±3	55±6	0.8±0.004	-11±4	39±12	50±17
Annual total	**-865±61**	**794±37**	**1658±106**	**-443±39**	**461±36**	**903±76**	**13±0.06**	**-708±58**	**681±153**	**1389±211**
Dec-13	-29±4	53±2	82±7	-23±2	31±2	54±4	0.7±0.004	-12±4	34±10	45±14
Jan-14	-30±5	51±3	80±8	-19±2	32±3	51±5	0.5±0.002	-28±4	45±9	73±13
Feb-14	-29±5	55±3	84±9	-22±1	28±2	49±4	0.8±0.002	-64±4	42±9	105±13
Mar-14	-64±5	84±3	147±8	-34±2	40±2	73±5	0.6±0.002	-55±4	76±16	130±21
Apr-14	-119±5	127±3	245±9	-46±3	55±3	100±6	0.6±0.004	-73±4	88±12	160±17
May-14	-136±5	141±3	276±9	-39±3	58±3	97±6	0.6±0.004	-64±5	121±13	185±18
Jun-14	-125±1	101±0	226±2	-48±2	53±2	101±4	0.6±0.001	-64±1	134±5	198±6
Jul-14	-131±4	68±3	198±8	-45±2	41±2	86±4	0.6±0	-89±5	83±20	172±26
Aug-14	-125±5	67±3	191±9	-34±2	41±1	75±4	0.5±0.009	-75±5	52±17	126±23
Sep-14	-81±5	68±3	148±8	-32±4	39±4	71±8	0.4±0.006	-77±6	64±19	140±25
Oct-14	-62±5	67±3	129±8	-24±2	32±2	56±4	0.4±0.007	-51±3	48±4	98±8
Nov-14	-32±4	68±2	99±7	-16±3	26±3	41±6	0.6±0.001	-27±3	46±11	72±14
Annual total	**-956±60**	**954±37**	**1909±97**	**-377±33**	**481±33**	**858±66**	**7±0.04**	**-673±54**	**837±150**	**1509±205**

[1] Units are g C /m2 month or g C /m2 year for net ecosystem exchange (NEE), respiration (Re), gross exchange (GEE) and methane production (CH4).

Table 5. ET, NEE and WUE at the flux stations.

Site	**ET**[1]	**-NEE**[2]	**WUE**[3]
Pine Upland	1050(yr1 [4]) 1070 (yr2 [5])	-700(yr1 [4]) -700 (yr2 [5])	0.7 / 1.0 (yr1 [4]) 0.7 / 1.0 (yr2 [5])
Dwarf Cypress	970(yr1 [4]) 900 (yr2 [5])	-450(yr1 [4]) -400 (yr2 [5])	0.5 / 0.7 (yr1 [4]) 0.4 / 0.7 (yr2 [5])
Cypress Swamp	1000(yr1 [4]) 1100 (yr2 [5])	-900(yr1 [4]) -1000 (yr2 [5])	0.9 / 1.4 (yr1 [4]) 0.9 / 1.4 (yr2 [5])

[1] Units are millimeters per year

[2] Units are g C per year

[3] Units are g C per millimeter ET or (/) moles CO_2 per mole ET

[4] yr1 from 12/1/2012 to 11/30/2013.

[5] yr2 from 12/1/2013 to 11/30/2014.

Table 6. Comparison of annual totals for NEE for different studies.

Ecosystem	**NEE**[1]	**Climate**	**Reference**
Taylor Slough (short sawgrass)	-50	Subtropics	Schedlbauer (2010)
Shark River Slough (short sawgrass)	45	Subtropics	Jimenez (2012)
Mangrove	-1170	Subtropics	Barr (2010)
Cypress Swamp	-900 to -1000	Subtropics	This study
Dwarf Cypress	-400 to -500	Subtropics	This study
Pine Upland	-750 to -800	Subtropics	This study
White Oak	-296	Temperate	Botkin (1070)
Scarlet Oak	-274	Temperate	Botkin (1070)
Pitch Pine	-124	Temperate	Botkin (1070)
Everglades	-100 to > -200	Subtropics	Jones et al. (2014)

[1] Units are g C per m^2 year

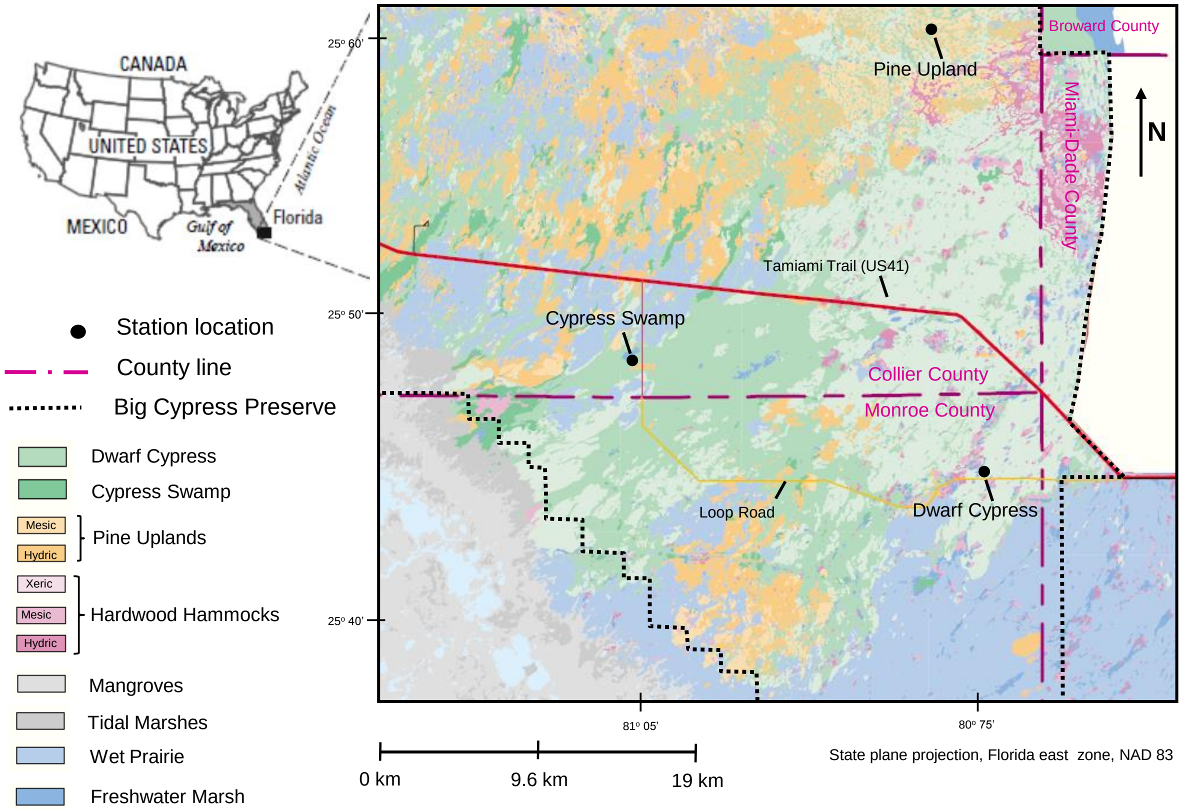

Figure 1. Location of the study area and vegetation communities, modified from Duever (2002).

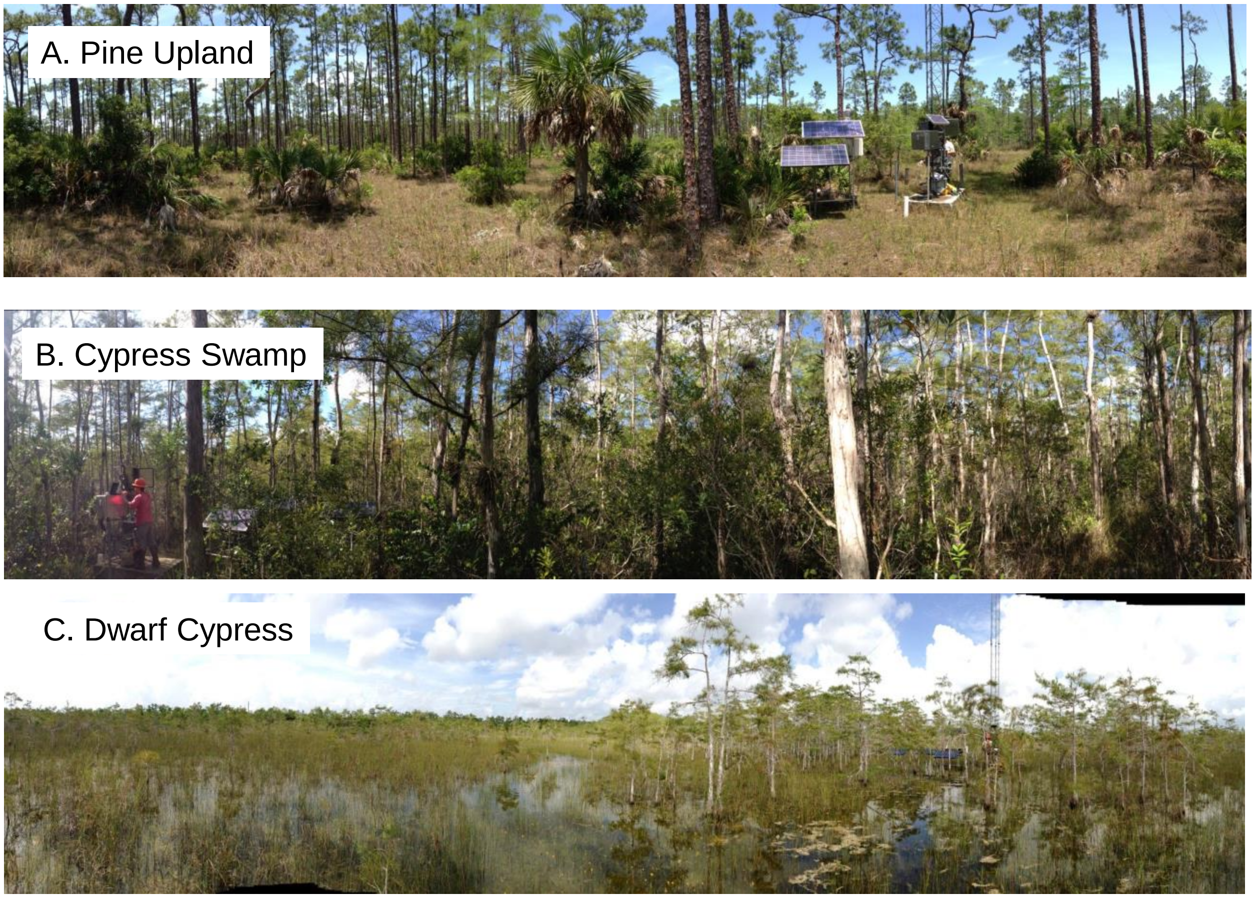

Figure 2. Panoramic photos of the (A) Pine Upland, (B) Cypress Swamp, and (C) Dwarf Cypress plant communities.

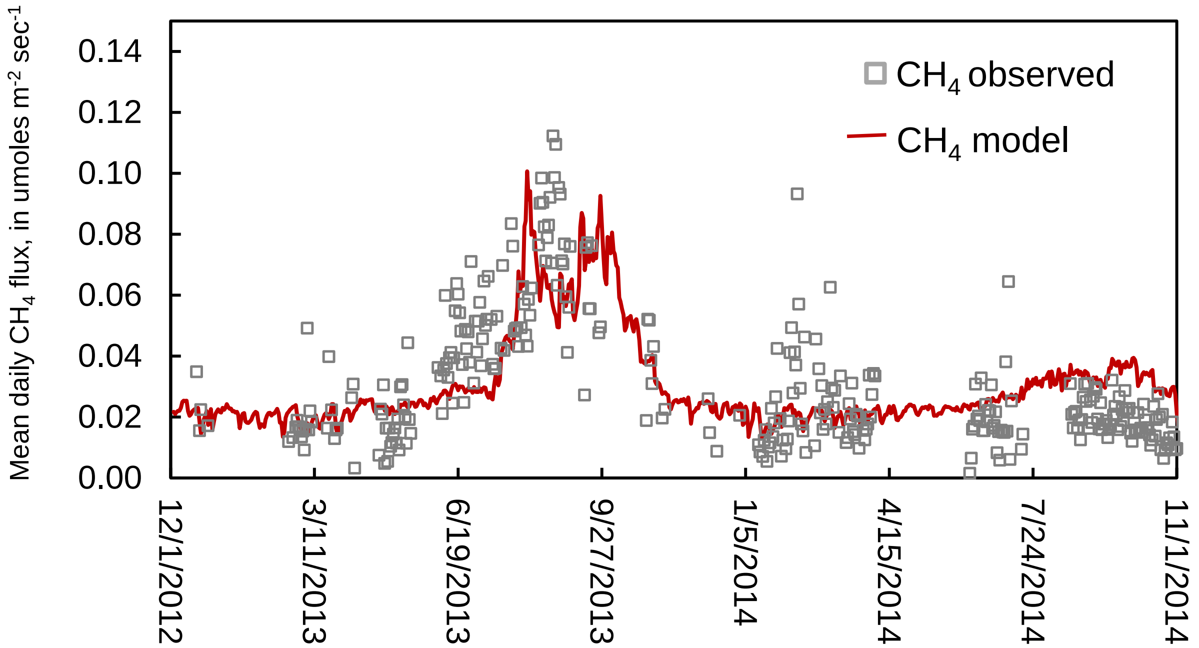

Figure 3. Observed and computed mean daily molar methane (CH4) flux at the Dwarf Cypress site.

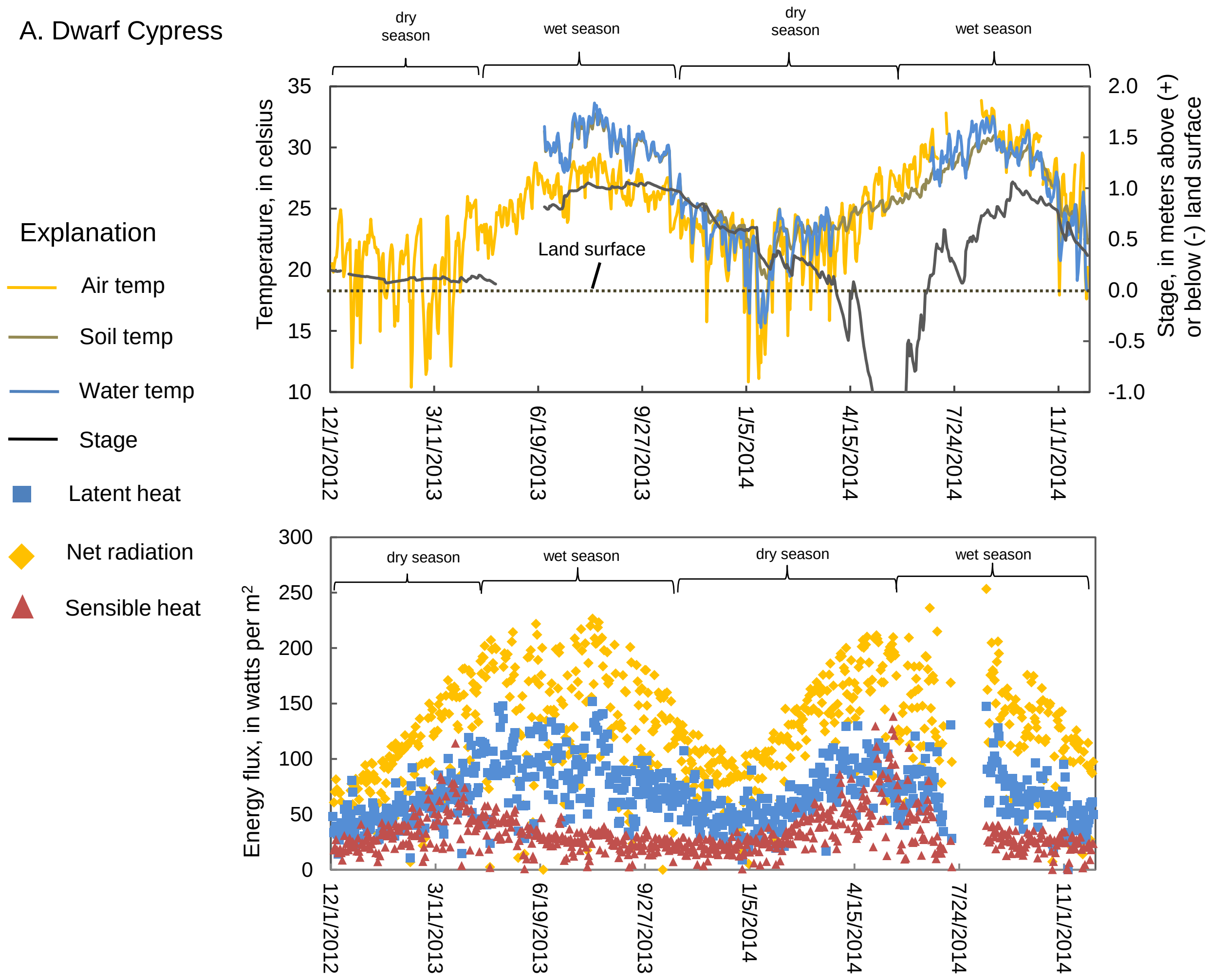
A. Dwarf Cypress
Explanation
Air temp
Soil temp
Water temp
Stage
Latent heat
Net radiation
Sensible heat
dry season
wet season
dry season
wet season
Land surface
Temperature, in celsius
35
30
25
20
15
10
Stage, in meters above (+) or below (-) land surface
2.0
1.5
1.0
0.5
0.0
-0.5
-1.0
12/1/2012
3/11/2013
6/19/2013
9/27/2013
1/5/2014
4/15/2014
7/24/2014
11/1/2014
Energy flux, in watts per m^2
300
250
200
150
100
50
0

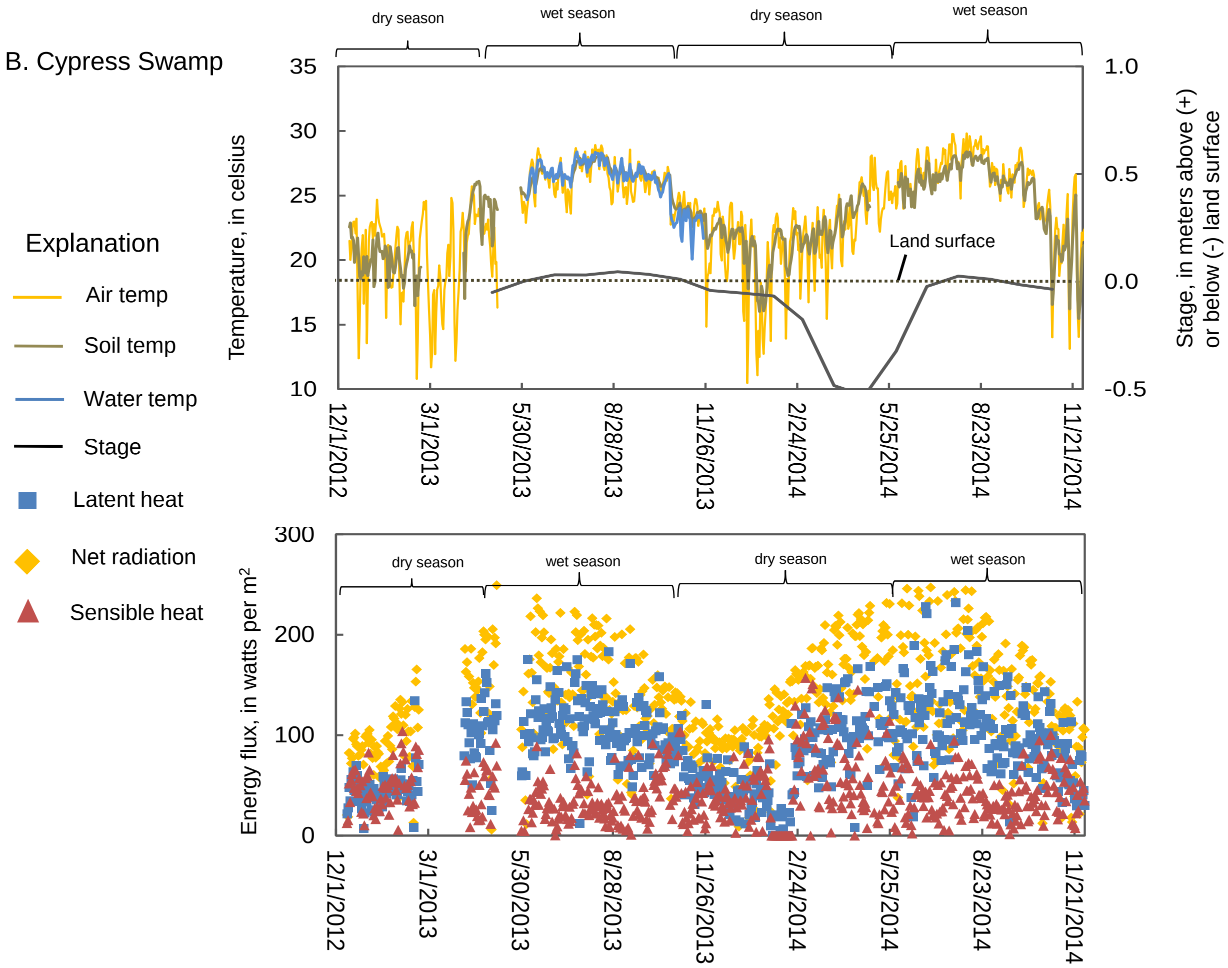
B. Cypress Swamp
Explanation
Air temp
Soil temp
Water temp
Stage
Latent heat
Net radiation
Sensible heat
dry season
wet season
dry season
wet season
Temperature, in celsius
35
30
25
20
15
10
Stage, in meters above (+) or below (-) land surface
1.0
0.5
0.0
-0.5
Land surface
12/1/2012
3/1/2013
5/30/2013
8/28/2013
11/26/2013
2/24/2014
5/25/2014
8/23/2014
11/21/2014
Energy flux, in watts per m^2
300
200
100
0
dry season
wet season
dry season
wet season
12/1/2012
3/1/2013
5/30/2013
8/28/2013
11/26/2013
2/24/2014
5/25/2014
8/23/2014
11/21/2014

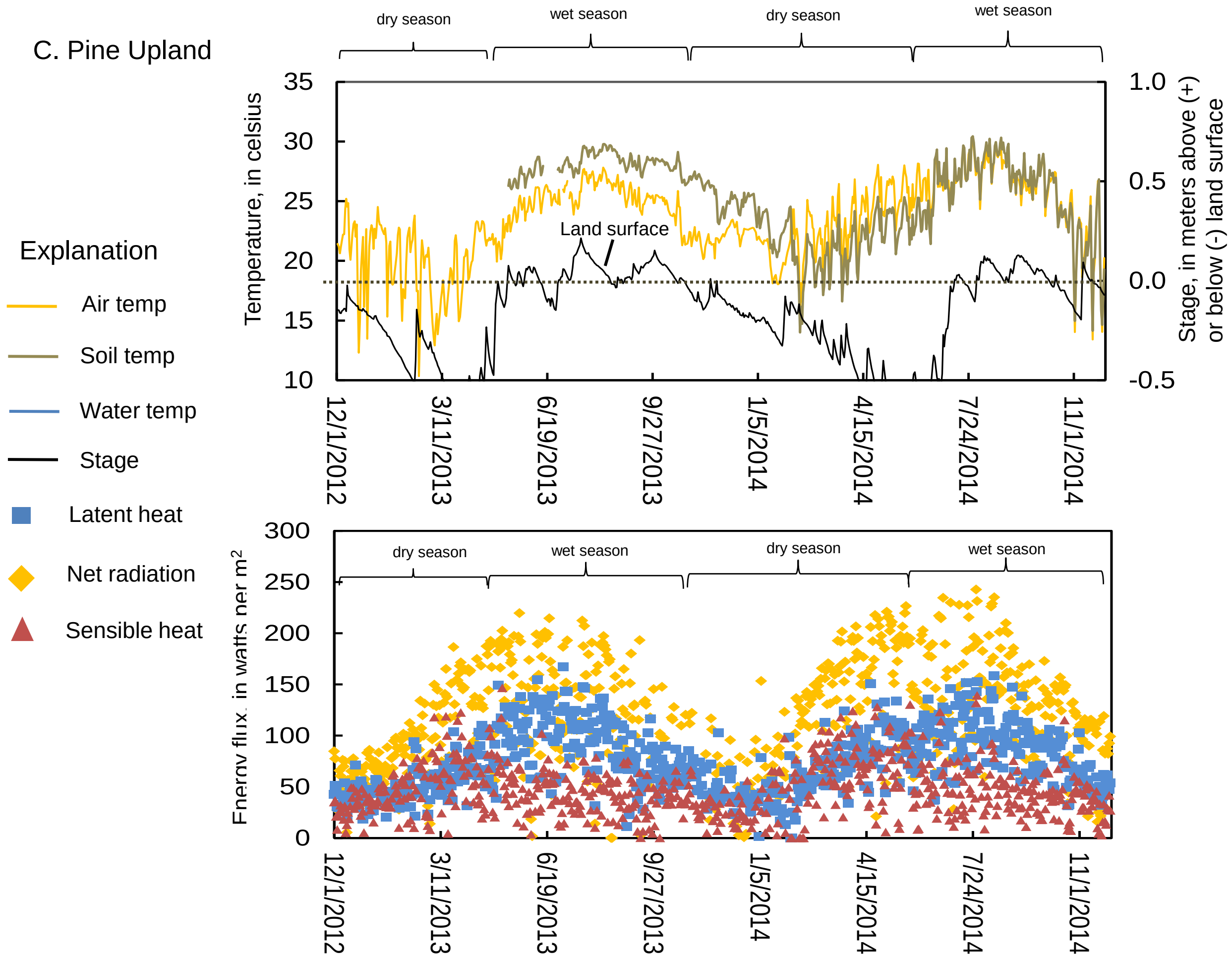

Figure 4A, B, C. Mean daily temperature and surface energy fluxes.

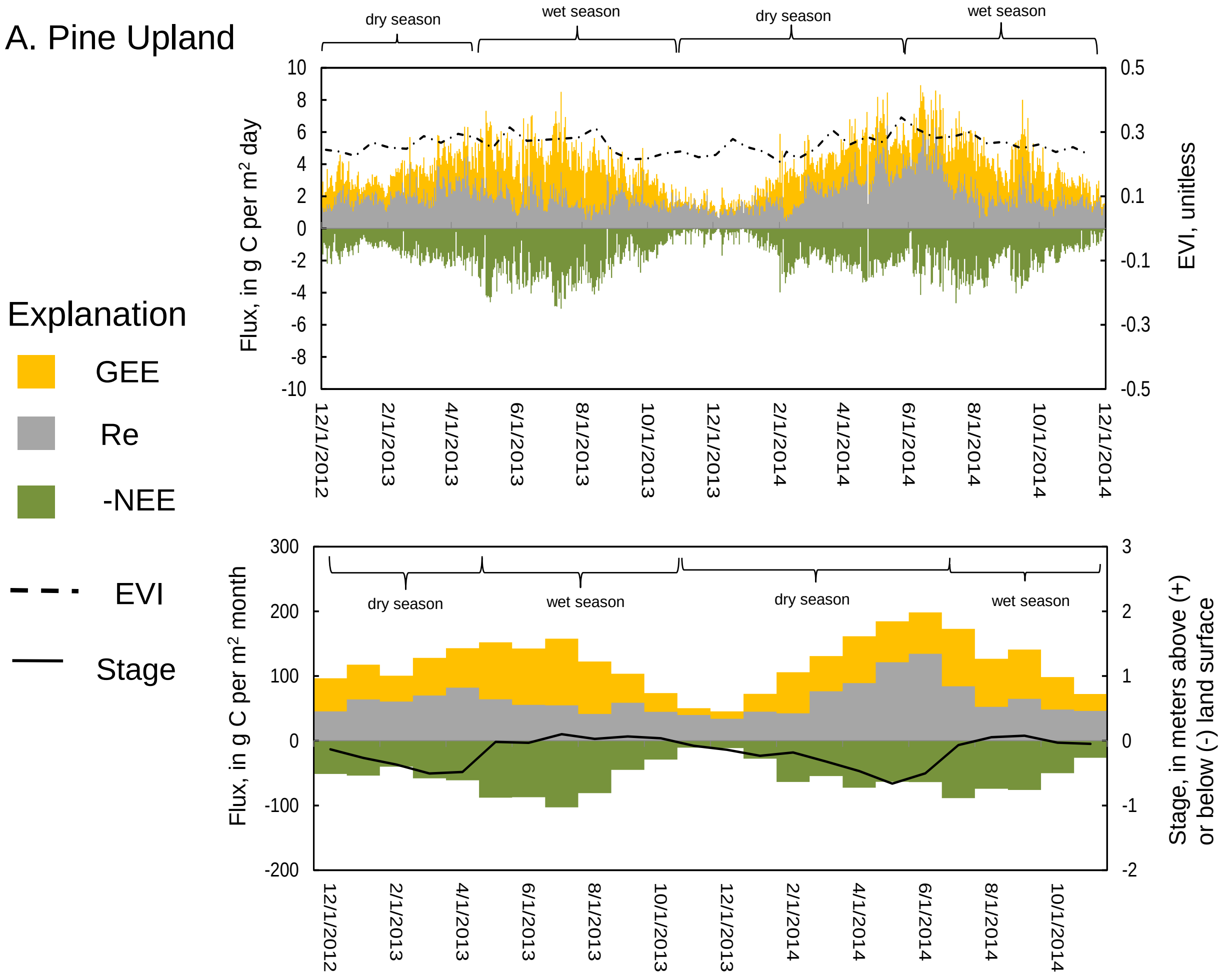
A. Pine Upland
Explanation
🟨 GEE
⬜ Re
🟩 -NEE
EVI
Stage
dry season
wet season
dry season
wet season
Flux, in g C per m^2 day
EVI, unitless
10
8
6
4
2
0
-2
-4
-6
-8
-10
0.5
0.3
0.1
-0.1
-0.3
-0.5
12/1/2012
2/1/2013
4/1/2013
6/1/2013
8/1/2013
10/1/2013
12/1/2013
2/1/2014
4/1/2014
6/1/2014
8/1/2014
10/1/2014
12/1/2014
Flux, in g C per m^2 month
Stage, in meters above (+) or below (-) land surface
300
200
100
0
-100
-200
3
2
1
0
-1
-2
dry season
wet season
dry season
wet season
12/1/2012
2/1/2013
4/1/2013
6/1/2013
8/1/2013
10/1/2013
12/1/2013
2/1/2014
4/1/2014
6/1/2014
8/1/2014
10/1/2014

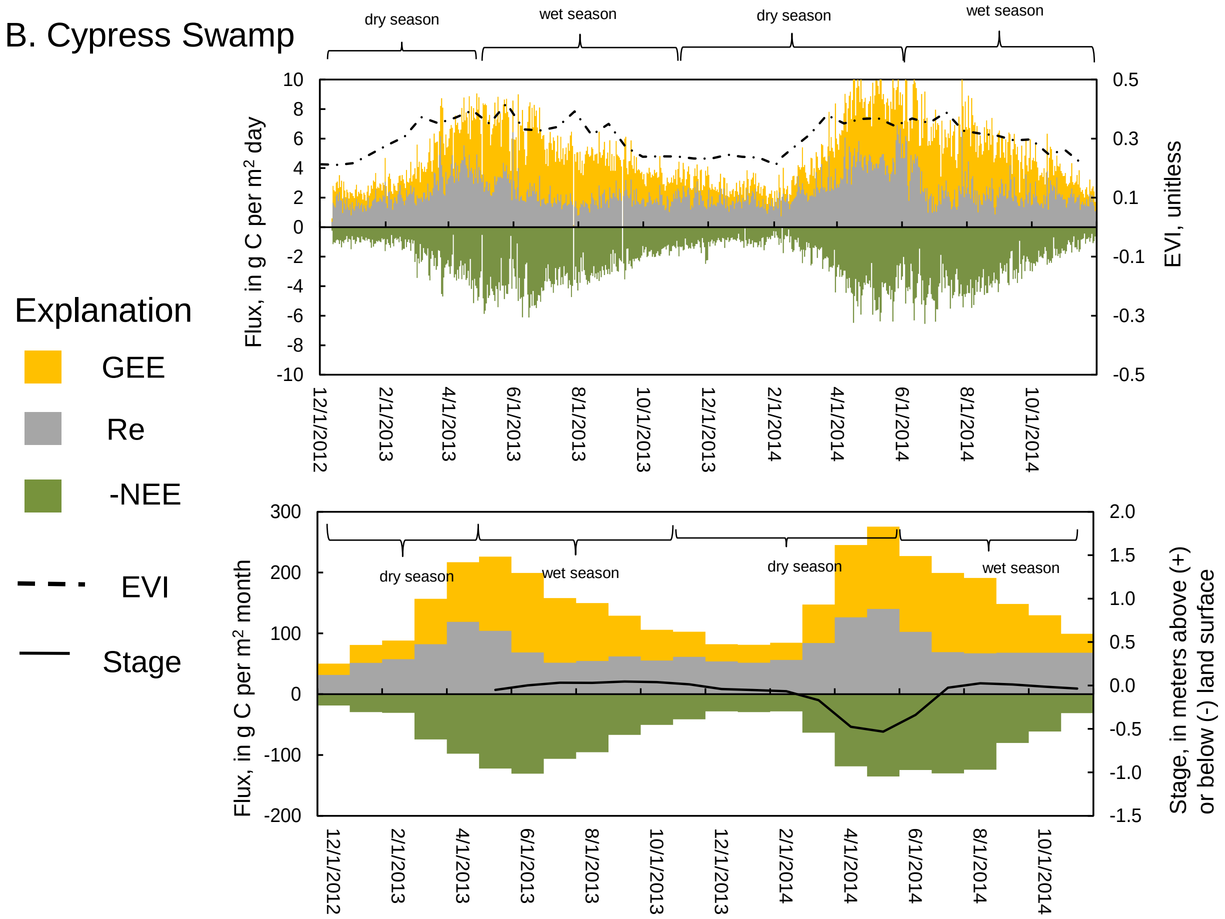
B. Cypress Swamp
dry season
wet season
dry season
wet season
Flux, in g C per m² day
EVI, unitless
10
8
6
4
2
0
-2
-4
-6
-8
-10
0.5
0.3
0.1
-0.1
-0.3
-0.5
12/1/2012
2/1/2013
4/1/2013
6/1/2013
8/1/2013
10/1/2013
12/1/2013
2/1/2014
4/1/2014
6/1/2014
8/1/2014
10/1/2014
Explanation
GEE
Re
-NEE
EVI
Stage
Flux, in g C per m² month
Stage, in meters above (+) or below (-) land surface
300
200
100
0
-100
-200
2.0
1.5
1.0
0.5
0.0
-0.5
-1.0
-1.5
dry season
wet season
dry season
wet season
12/1/2012
2/1/2013
4/1/2013
6/1/2013
8/1/2013
10/1/2013
12/1/2013
2/1/2014
4/1/2014
6/1/2014
8/1/2014
10/1/2014

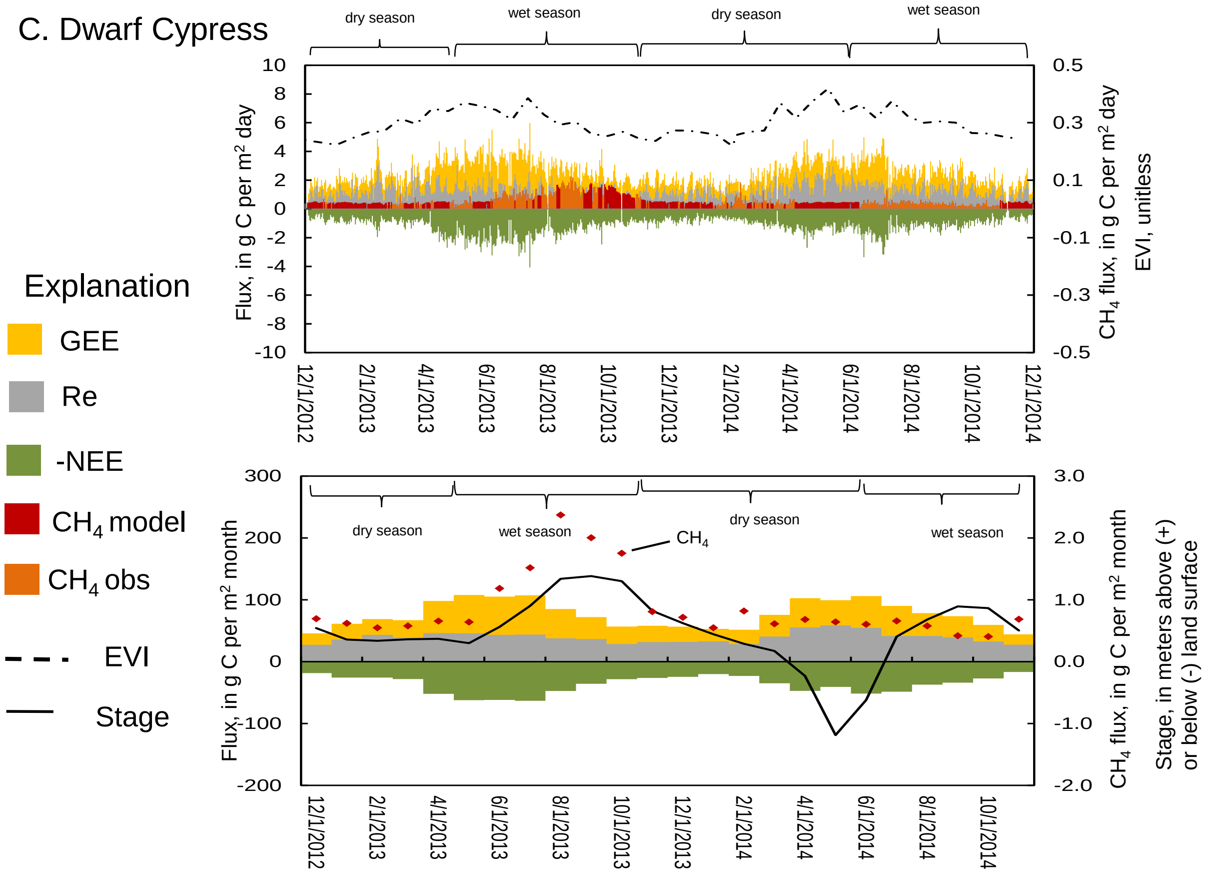

Figure 5A, B, C. Daily and monthly C fluxes, stage and EVI at the (A) Pine Upland, (B) Cypress Swamp and (C) Dwarf Cypress sites.

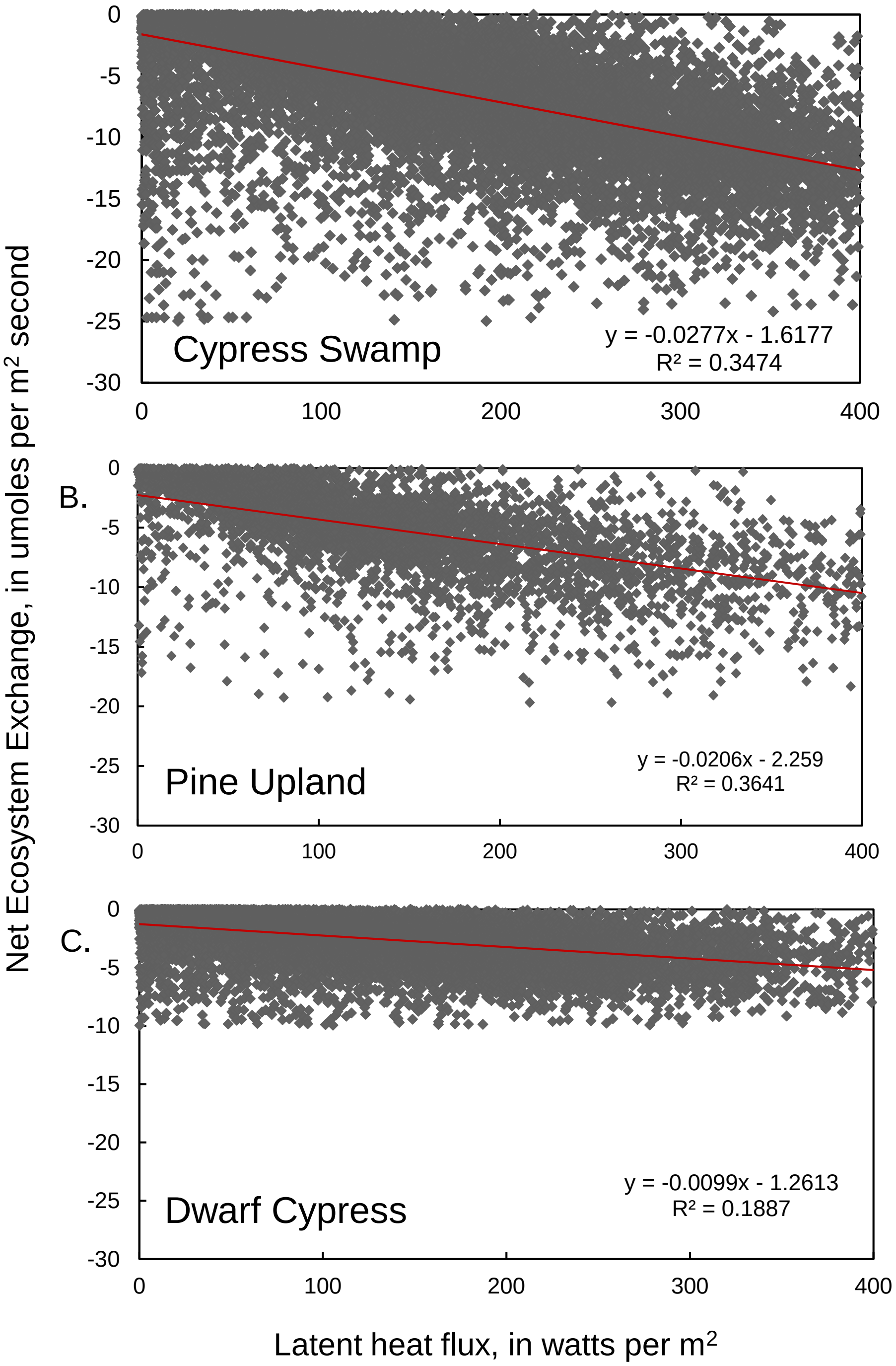

Figure 6. Relations between latent heat flux and net ecosystem exchange.